Journal of Materials Chemistry C

RSC Publishing

PAPER

View Article Online
View Journal | View Issue

Cite this: J. Mater. Chem. C, 2013, 1, 7453

A plano-convex/biconvex microlens array based on self-assembled photocurable polymer droplets

Hongwen Ren,*[a] Su Xu,[b] Yifan Liu[b] and Shin-Tson Wu*[b]

Received 2nd July 2013
Accepted 8th September 2013

DOI: 10.1039/c3tc31268b

www.rsc.org/MaterialsC

We report the performance of a plano-convex/biconvex microlens array (MLA) fabricated using self-assembled photocurable polymer droplets. The morphologies of the microlens arrays are examined by SEM and AFM, and the imaging characteristics are evaluated using an optical microscope. The demonstrated MLAs possess the following advantages: simple fabrication procedure, good flexibility, and good optical performance. By properly controlling the filled monomer, MLAs with high fill factor and large numerical aperture are obtainable. Our polymeric MLA enables an easy integration with existing photonic devices and has promising applications in light diffusers, fiber/organic LED couplers, 3D micro-projection displays, and biomedical imaging.

Introduction

As the miniaturization of optical systems advances, microlens arrays (MLA) have become essential components for image processing, fiber coupling, optical data storage, light extraction, diffusers, displays, and biomedical inspection. Various fabrication methods of MLAs have been developed, such as laser ablation,[1] lithography,[2] grayscale masking,[3,4] thermal reflow,[5–7] elastomeric stamps,[8–10] molding,[11–14] phase separation,[15] and so on.[16–19] However, these approaches often involve sophisticated fabrication procedures as well as lengthy production processes. So far, only plano-convex lenses have been demonstrated. Moreover, most MLAs are fabricated on a solid substrate, which has limited flexibility. A small numerical aperture (NA: 0.1–0.3) is another problem as it leads to a fairly low resolution.

The lens shape plays a critical role in minimizing optical aberrations. Generally speaking, plano-convex is desirable when working at or near infinity conjugate (collimated light on one side of the lens), while biconvex MLAs exhibit a minimum aberration at conjugate ratios between 5 : 1 and 1 : 5. Therefore, biconvex MLAs are preferred for a finite conjugate, *e.g.*, imaging processing, illumination, and displays. But it would be a big challenge for the above mentioned approaches to obtain biconvex MLAs. To overcome this issue while keeping the advantages of a simple fabrication procedure, good flexibility after peeling off, and high NA, a new fabrication strategy is urgently needed.

Previously, we have demonstrated an adaptive liquid MLA by patterning a polymer film with cavities and filling these cavities with a dielectric liquid.[20] Due to surface tension, the liquid could be self-assembled into each cavity, forming a droplet with a plano-convex lens character. Such a liquid MLA needs two glass substrates to form a lens frame. To minimize the gravity effect and liquid evaporation, the chamber is filled with another immiscible liquid and tightly sealed. The liquid medium offers a tunable optical power, but the rigid glass frame limits its flexibility.

In this paper, we report a rapid fabrication of polymeric MLAs through patterning a polymer film with cavities and filling these cavities with a photocurable monomer. Similar to our liquid MLAs, due to surface tension the monomer could be self-assembled into each cavity to form a lens shape. After solidification *via* photo-polymerization, a plano-convex/biconvex polymeric MLA is obtained. By properly controlling the filled monomer, polymeric MLAs with high fill factor, good optical performance, and large NA are feasible. All of these properties are well maintained even after the MLA film is peeled off from the glass substrate. Our polymeric MLAs enable an easy integration with existing photonic devices for a wide variety of applications.

Fabrication procedures and mechanism

Fabrication procedures

Fig. 1 depicts the schematic diagram for fabricating a plano-convex MLA. Firstly, we spin-coated a thin photocurable monomer layer onto a glass substrate (Fig. 1(a)) and then applied UV irradiation through a photomask from the bottom (Fig. 1(b)). Those monomers in the unexposed areas are not cured and can be removed easily by rinsing the film with a solvent (such as ethanol). As a result, a polymeric film with cavities remains on the glass substrate (Fig. 1(c)). Secondly, we treated the film surface with Teflon solution (surface tension $\sim$ 18 mN m^{-1}), which was initially spin-coated onto a glass

[a]Department of Polymer Nano Science and Technology, Chonbuk National University, Jeonju, Jeonbuk, South Korea. E-mail: hongwen@jbnu.ac.kr; Fax: +82-63-270-2341; Tel: +82-63-270-2354

[b]College of Optics and Photonics, University of Central Florida, Orlando, Florida, USA. E-mail: swu@ucf.edu; Fax: +1 407-823-6880; Tel: +1 407-823-4763

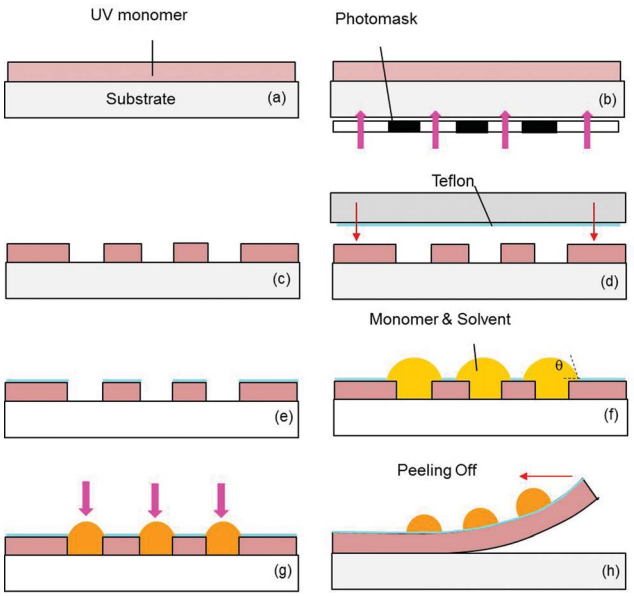

Fig. 1 Fabrication procedures of a plano-convex polymeric MLA. (a) Coating a liquid monomer layer on a glass substrate. (b) UV curing through a photomask. (c) Forming a cavity array by removing the uncured monomers with a solvent. (d) Coating a Teflon layer on a glass substrate and stamping it on the polymer film surface. (e) The surfactant is transferred to the polymer film surface. (f) Filling a monomer mixture into the cavities. (g) Evaporating the solvent and UV curing the monomer droplets. (h) Peeling off the MLA film.

substrate (Fig. 1(d)) and subsequently transferred to the film through stamping (Fig. 1(e)). Thirdly, we filled the cavities with a mixture of liquid monomer and low surface-tension solvent (Fig. 1(f)). Here the low surface-tension solvent serves two purposes: decreasing the surface tension of the monomer for easy cavity-filling and controlling the monomer amount in each cavity. When a small amount of the mixture is dripped on the film surface and gently laminated using a glass rod, each cavity traps a certain amount of the mixture, and meanwhile, the Teflon layer prevents the mixture from aggregating on the film surface (Fig. 1(f)). Therefore, monomer droplets are only formed in the cavities after thoroughly evaporating the solvent (Fig. 1(g)). Finally, we solidified these droplets *via* photo-polymerization. Because the droplet array is firmly fixed in the cavities, we can peel off the polymeric film from the glass substrate and obtain a thin flexible polymer MLA (Fig. 1(h)).

Mechanism

The physical mechanisms responsible for the above-mentioned fabrication procedures are explained as follows. When a liquid falls on a solid surface, the formed droplet may wet, partially wet, or not wet the solid surface, depending on the surface tension. Let us assume that the liquid droplet is in an equilibrium state with a laterally symmetric surface profile, as shown in Fig. 2(a). Because of the surface tension between liquid and solid surrounded by vapor, the droplet exhibits a contact angle on the solid surface, which is expressed by Young's equation,[21]

$$\cos\theta = (\gamma_{SV} - \gamma_{SL})/\gamma_{LV} \quad (1)$$

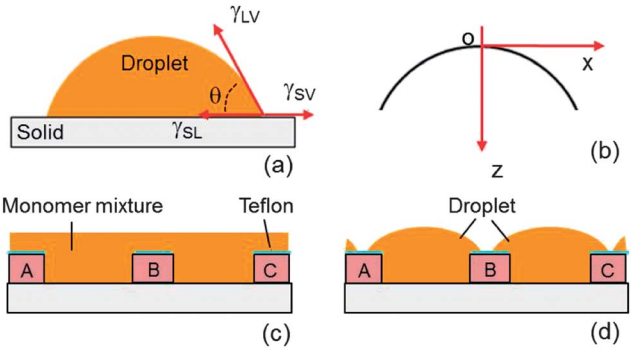

Fig. 2 (a) Definition of contact angle when a liquid droplet falls on a solid substrate surface. (b) Illustration of the droplet surface profile in the *XZ* coordinate system. (c) The filled monomer mixture initially has a quasi-flat surface. (d) The monomer mixture breaks into uniform droplets due to surface tension.

where γ_{SL}, γ_{SV}, and γ_{LV} are solid–liquid, solid–vapor, and liquid–vapor interfacial tensions, respectively, and θ is the equilibrium contact angle. In eqn (1), we find that decreasing γ_{SV} and γ_{SL} will cause θ to increase, which means that the droplet would contract. Coating Teflon onto the polymer film surface is a simple way to increase the contact angle [Fig. 1(g)]. If the droplet surface is treated as an ultra-thin elastic membrane, then in a coordinate *XZ* system, the 2D droplet shape can be expressed as[22,23]

$$Z = P(a^2 - x^2)/4\gamma_{LV} \quad (2)$$

where a is the radius of the droplet aperture and P is the pressure difference across the droplet surface. If the ambient temperature and pressure are kept unchanged, P and γ_{LV} will not change either. From eqn (2), the droplet presents a parabolic shape due to the axial symmetry, as shown in Fig. 2(b). In comparison to a spherical lens, the parabolic lens usually presents less spherical aberration. The formation of a MLA shown in Fig. 1(f) is well explained in Fig. 2(c) and (d). When the monomer mixture is laminated on the surface of the polymer film, the cavities can be fully filled and the top surface of the mixture is quasi-flat because of its relatively low surface tension, as depicted in Fig. 2(c). As the solvent evaporates, the mixture near the border of the cavities (indicated by A, B, and C) touches the Teflon surface first, and meanwhile the surface tension of the mixture has a tendency to increase. As a result, the mixture begins to break into disconnected pieces from these areas. The monomer in each cavity continues to shrink with the ongoing evaporation. Finally, the liquid monomer partially wets the Teflon surface with a contact angle so that a plano-convex lens is formed (Fig. 2(d)).

Experiments and discussions

Plano-convex microlens array

To prove the concept, in experiment we first prepared a plano-convex MLA according to the fabrication procedures outlined in Fig. 1. We spin-coated NOA65 (refractive index $n = 1.524$, surface tension $\gamma \sim 40$ mN m^{-1} at 25 °C) onto a glass substrate

(thickness: 120 μm). NOA65 is a clear liquid photopolymer, which is curable under UV light ($\lambda \sim 365$ nm). The photomask we employed has an octagon–chrome-spot-array pattern, in which the diameter of each octagon spot and the space between adjacent spots are 50 μm and 8.5 μm, respectively (Fig. 3(a)). The UV exposure lasts for 20 seconds at an intensity of 20 mW cm^{-2}. A polymer cavity array was obtained after rinsing and drying. The aperture shape and uniformity were observed under an optical microscope (OM), as shown in Fig. 3(b). The black spots are the formed cavities. Then the film surface was treated with Teflon through a transferring method, followed by drying. A mixture of 85 wt% NOA65 and 15 wt% acetone ($\gamma \sim 23$ mN m^{-1} at 24 °C) was laminated on the film surface. After thoroughly evaporating the acetone, the droplet array was fully cured *via* UV exposure. Fig. 3(c) shows the image of the droplets observed under the OM, and the inset is a magnified image of four microlenses. The observed droplet image is in the defocused state because their surface is not flat. For comparison, one cavity was intentionally left unfilled, as indicated by the purple arrow in Fig. 3(c).

The fabricated MLA film can stand alone without any substrate after peeling off from the glass substrate (Fig. 3(d)). The effective MLA area is 4 cm × 4 cm. The focusing ability was inspected under the OM. By adjusting the stage position, the incident light was well focused into a circular spot array (Fig. 3(e)). Such a result implies that each droplet indeed functions as a converging microlens. A weak light leakage is also observed, which comes from the corner of each cavity, as indicated in Fig. 3(c). This can be eliminated by fabricating a black polymer film with cavities (*e.g.*, adding black dyes into NOA65 before spin-coating). For a MLA, both NA and fill factor are important parameters affecting the overall light efficiency. When a lens is focused at infinity, the image-space NA of the lens can be approximated by[24]

$$\mathrm{NA} \sim D/2f \tag{3}$$

where D is the effective diameter of the microlens and f is the focal length. The focal length of the MLA can be estimated through the OM measurement. At first, we adjusted the stage until seeing a clear image of the droplet surface (Fig. 3(c)), and then adjusted the stage to get a clear image of the focal point (Fig. 3(e)). Comparing the focal length with the object distance, the position of the object can be assumed as infinity. Thus the distance between these two stage positions can be considered as the focal length of the microlens. Here the average focal length and effective diameter were measured to be ~58 μm and ~53 μm, respectively, and the NA was estimated to be ~0.46. In our prepared MLA, each cavity is fully occupied by a droplet and the space between adjacent droplets is quite limited except the corner regions. The fill factor is calculated to be ~75%. By designing a photomask with narrower corner regions and filling more mixture into each cavity, the fill factor can be further increased.

The surface profile of the MLA was further verified using a scanning electron microscope (SEM). The top-view and oblique-view of our MLA are displayed in Fig. 4(a) and (b), respectively. These droplets present a smooth plano-convex lens shape with a circular aperture. During the oblique-view observation, the MLA film was both horizontally and vertically tilted, in order to take a picture including more microlenses. Otherwise, only the most

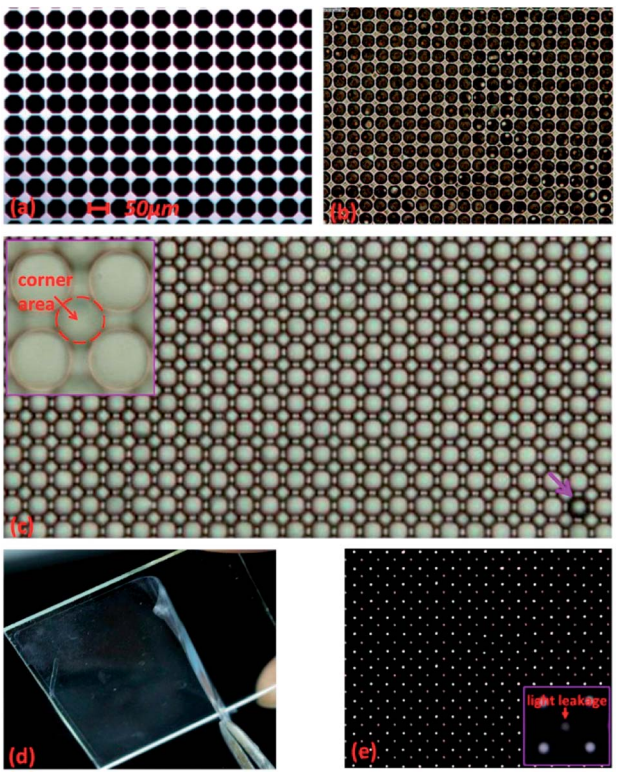

Fig. 3 Optical images of (a) the photomask with an octagon–chromium-spot-array pattern, (b) the polymer cavity array, (c) a cured droplet array in the cavities with one unfilled cavity (indicated by the purple arrow), the inset shows the corner area among four microlenses in the defocus state, (d) peeling off the MLA film from the glass substrate, and (e) a focused spot array under white illumination, the inset is a magnified image indicating light leakage.

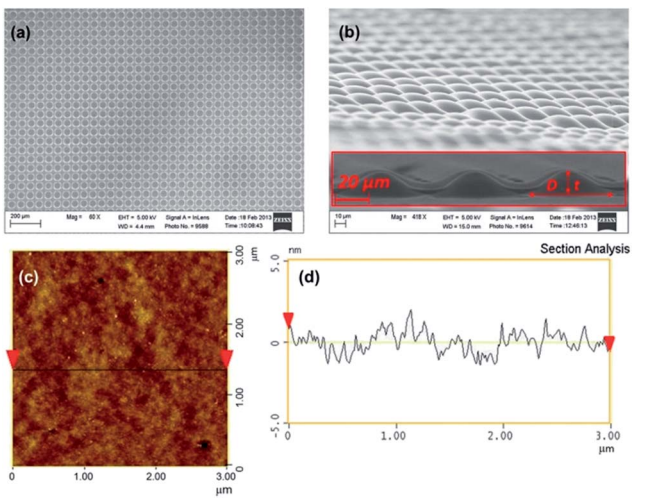

Fig. 4 (a) Top-view SEM image of MLA (60× magnification). (b) Oblique-view SEM image of MLA (418× magnification) and a side-view inset. AFM images of (c) topography of a solid droplet with a 3 × 3 μm^2 scanning area, and (d) cross-sectional surface profile between two red triangles.

front ones are observed while those in the back are blocked, as shown in the side-view inset in Fig. 4(b). This also explains why the microlens shape varies somewhat in Fig. 4(b) and the inset. Based on the SEM images, the microlens aperture D was measured to be ~53 μm and the droplet's apex distance $t \sim 15$ μm. Given the refractive indices of NOA65 ($n_{NOA} \sim 1.524$) and air ($n_a \sim 1$), the focal length is calculated to be $f \sim 59$ μm and thus NA is ~0.45. These results agree well with those estimated using the OM. It should be noted that once the filled NOA65 monomer forms a droplet in the cavities, it shows a perfect plano-convex lens shape due to its fairly high surface tension (40 mN m^{-1}). Furthermore, no obvious degradation in the surface smoothness is observed after UV polymerization, as determined by the atomic force microscopy (AFM) image of one polymerized droplet. Fig. 4(c) shows the surface topography of a 3×3 μm^2 scanned area. The other area of the droplet surface presents a similar morphology. Fig. 4(d) illustrates the surface roughness of a cross-sectional surface profile along the segment marked by two triangles in Fig. 4(c). The root mean square (RMS) and maximal roughness (R_{max}) of the surface are ~0.67 and ~3.55 nm, respectively. Compared with a green wavelength at $\lambda \sim 550$ nm, such a roughness is negligible and does not degrade the lens performance.

Bi-convex microlens array

In addition to plano-convex MLAs, we can also use the proposed method to fabricate a biconvex MLA fairly easily, as shown in Fig. 5. Firstly, we prepared a cavity film with a Teflon-treated top surface (Fig. 5(a)–(d)) and the procedures were exactly the same as those shown in Fig. 1(a)–(d). Then we peeled off the film from the glass substrate (Fig. 5(e)) and stamped its bottom surface on another glass substrate with a spin-coated Teflon layer (Fig. 5(f)). In this way, both surfaces of the polymer were treated with Teflon. The film was placed on an elastic holder and the cavities were filled with the NOA65/acetone mixture (Fig. 5(g)). Since the inner surface of the polymer cavity was not coated with Teflon, the cavity wall strongly attracted the mixture. After the solvent was completely evaporated, the remained monomer droplet exhibited a biconvex shape and solidified *via* UV exposure (Fig. 5(h)).

The optical performance of this biconvex MLA was also evaluated using an optical microscope. A small letter "A" typed on a piece of transparency was adopted as an object. Through adjusting the stage position, the MLA imaged the object to an array of inverted "A" under white light illumination (Fig. 6(a)). Some displayed images were slightly blurred because the film was not perfectly flat when placed on the holder. The average aperture and focal length were measured to be ~50 μm and 48 μm, and thus NA was calculated to be ~0.52. Fig. 6(b) shows the image of a 1951 U.S. Air Force (USAF) resolution target taken through one biconvex microlens, which indicates a ~40 lp mm^{-1} resolution as the patterns of group 5 element 3 can still be clearly resolved.

The biconvex surface profile of the MLA is confirmed by SEM. Fig. 7(a) shows the SEM image of its top surface and the inset is a magnified image. Fig. 7(b) shows the SEM image of its bottom surface and the inset is a magnified side-view. One can clearly see that the monomers only form droplets in the cavities

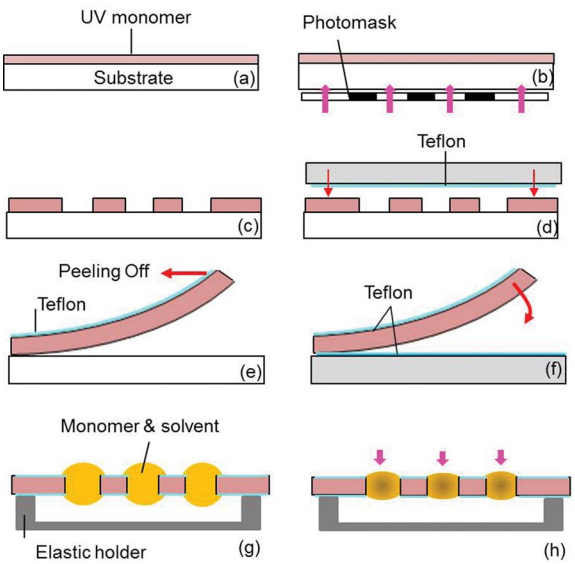

Fig. 5 The fabrication procedures of a biconvex MLA. (a) Coating a liquid monomer layer on a glass substrate. (b) UV curing through a photomask. (c) Forming a cavity array by removing the uncured monomers with a solvent. (d) Coating a Teflon layer on a glass substrate and stamping it on the polymer film surface. (e) Peeling off the polymer film from the glass substrate. (f) Treating the bottom surface of the film with Teflon through stamping it on a glass substrate coated with Teflon. (g) Placing the film on an elastic holder and filling a monomer mixture into the cavities. (h) Evaporating the solvent and UV curing the monomer droplets.

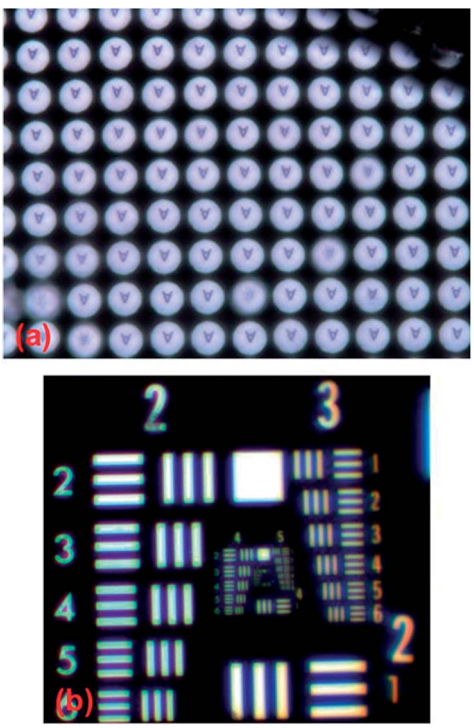

Fig. 6 Optical images of (a) an inverted "A" array observed through the biconvex MLA and (b) a resolution target observed through one biconvex microlens.

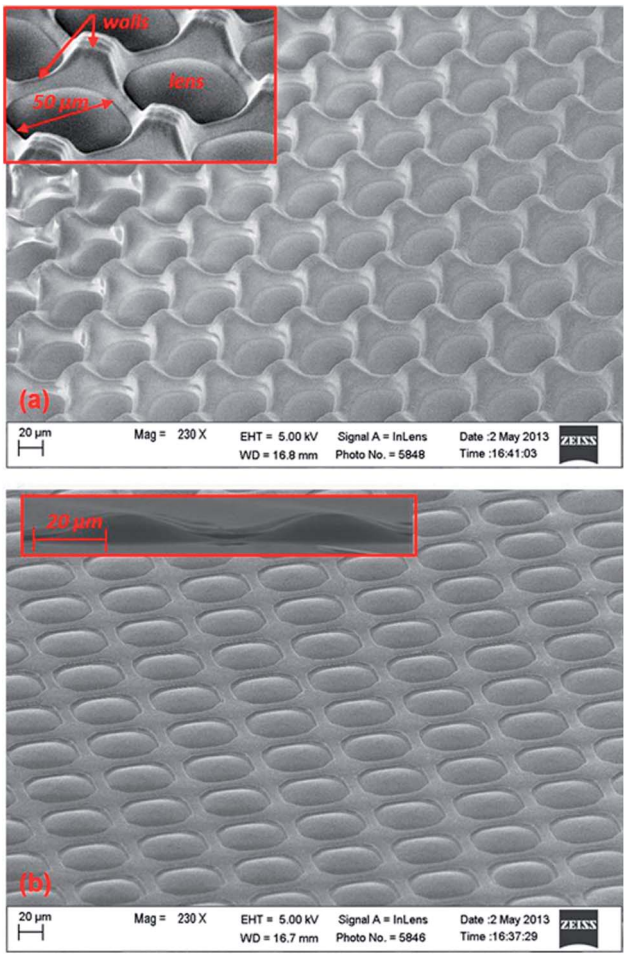

Fig. 7 SEM images of the biconvex MLA: (a) the top surface, the inset is a magnified image showing two microlenses, and (b) bottom surface, the inset is a side-view.

without any residual on the film surface. Each droplet is well separated by the cavity wall. However, by comparing the top and bottom surfaces of the polymer film, we found some subtle differences in surface tomography. The possible causes are twofold: (1) we intentionally fabricate a thick polymer film for easy transfer and Teflon treatment in the experiment. Compared with those located in the bottom (closer to the UV source), the monomers located in the top area (farther away from the UV source) experience weaker UV exposure due to light diffraction. They could not be fully polymerized if the UV dose could just polymerize the bottom. As a result, the cavity walls in the top surface have a wave-like structure (Fig. 7(a)). (2) Over exposure will also cause a shape difference between the top and the bottom opening of the cavity, *i.e.*, the top opening is larger than the bottom one. By controlling the film thickness and optimizing the exposure conditions, the difference in the two openings can be solved.

Our proposed method shows a number of competitive advantages. Firstly, it offers a possibility to fabricate both plano-convex and biconvex MLAs in a simple and rapid way. The fabricated MLAs have distinctive features such as good uniformity, large fill factor, and high optical performance. The microlens aperture and surface profile can be controlled by the photomask and the filled monomer amount, respectively. These two factors also affect the MLA's fill factor and NA. Secondly, the MLA film can be peeled off from the substrate without any obvious degradation in the optical performance and surface smoothness. Such flexible MLAs can be easily integrated with existing photonic devices for a wide variety of applications. Last but not least, aspherical MLAs can also be fabricated using our approach by introducing a dielectrophoretic force in the step shown in Fig. 1(f).[25] Although the Teflon layer is not fully baked, it still provides a good hydrophobic property. Low-baking-temperature Teflon helps to further optimize the hydrophobic properties of the polymer surface and enhance the contact angle.

Conclusions

In summary, we have demonstrated a simple and rapid method to fabricate polymeric microlens arrays (MLAs). By patterning a polymer film with cavities and filling these cavities with photosensitive monomers, the monomer droplet in each cavity presents a lens character, which can be solidified *via* UV exposure. Both plano-convex and biconvex MLAs were demonstrated. The fabricated plano-convex MLA has a numerical aperture NA ~0.45 and fill factor ~75%, and the biconvex MLA has a NA ~0.52 and resolution ~40 lp mm^{-1}. By properly controlling the filled monomer, our MLA exhibits a high fill factor, large NA, and good optical performance. All of these properties are well maintained even after the MLA film is peeled off from the glass substrate. The major advantages of our MLAs are simple fabrication, good uniformity, compactness, good flexibility after peeling off, and high optical performance. Through integrating with other photonic devices, our MLAs have promising applications in light diffusers, fiber/organic LED couplers, 3D micro-projection displays, and biomedical technologies.

Acknowledgements

H. Ren is supported by the National Research Foundation of Korea, the international joint research program under grant 20120004814 for the financial support. The University of Central Florida group is indebted to the U.S. Air Force Office of Scientific Research (AFOSR) for partial financial support under contract no. FA95550-09-1-0170.

References and notes

1 S. Mihailov and S. Lazare, *Appl. Opt.*, 1993, **32**, 6211.
2 R. J. Jackman, J. L. Wilbur and G. M. Whitesides, *Science*, 1995, **269**, 664.
3 M.-H. Wu, C. Park and G. M. Whitesides, *Langmuir*, 2002, **18**, 9312.
4 J.-J. Yang, Y.-S. Liao and C.-F. Chen, *Opt. Commun.*, 2007, **270**, 433.
5 D. Daly, R. F. Steven, M. C. Hutley and N. Davies, *Meas. Sci. Technol.*, 1990, **1**, 759.
6 Y. Lu, Y. Yin and Y. Xia, *Adv. Mater.*, 2001, **13**, 34.
7 A. Verma and A. Sharma, *Adv. Mater.*, 2010, **22**, 5306.

8 Y. Xia, J. Tien, D. Qin and G. M. Whitesides, *Langmuir*, 1996, **12**, 4033.
9 Y. Xia, E. Kim, X.-M. ZhaoJ, A. Rogers, M. Prentiss and G. M. Whitesides, *Science*, 1996, **273**, 347.
10 D. Kang, C. Pang, S. M. Kim, H. S. Cho, H. S. Um, Y. W. Choi and K. Y. Suh, *Adv. Mater.*, 2012, **24**, 1709.
11 Y. K. Shen, *Polym. Eng. Sci.*, 2006, **46**, 1797.
12 E. P. Chan and A. J. Crosby, *Adv. Mater.*, 2006, **18**, 3238.
13 K. H. Liu, M. F. Chen, C. T. Pan, M. Y. Chang and W. Y. Huang, *Sens. Actuators, A*, 2010, **159**, 126.
14 X. Li, Y. Ding, J. Shao, H. Tian and H. Liu, *Adv. Mater.*, 2012, **24**, OP165.
15 L.-C. Huang, T.-C. Lin, C.-C. Huang and C.-Y. Chao, *Soft Matter*, 2011, **7**, 2812.
16 Y. Lu, Y. Yin and Y. Xia, *Adv. Mater.*, 2001, **13**, 34.
17 J. Xia, D. Qu, H. Yang, J. Chen and W. Zhu, *Displays*, 2010, **31**, 186.
18 K. Lee, W. Wagermaier, A. R. Masic, K. P. Kommareddy, M. Bennet, I. Manjubala, S.-W. Lee, S. B. Park, H. Colfen and P. Fratzl, *Nat. Commun.*, 2012, **3**, 1.
19 J.-Y. Huang, Y.-S. Lu and J. A. Yeh, *Opt. Express*, 2006, **14**, 10779.
20 H. Ren, D. Ren and S.-T. Wu, *Opt. Express*, 2009, **17**, 24183.
21 T. Young, *Philos. Trans. R. Soc. London*, 1805, **95**, 65.
22 G. C. Knollman, J. L. Bellin and J. L. Weaver, *J. Acoust. Soc. Am.*, 1971, **49**, 253.
23 N. Sugiura and S. Morita, *Appl. Opt.*, 1993, **32**, 4181.
24 E. Hecht, *Optics*, Addison Wesley, New York, 4th edn, 2002.
25 K. Y. Hung, C. C. Fan, F. G. Tseng and Y. K. Chen, *Opt. Express*, 2010, **18**, 6014.